

Nutrients and dissolved oxygen in the upper 1000 m in equatorial western Indian Ocean

P V Shirodkar & D A Jayakumar

National Institute of Oceanography, Dona Paula, Goa 403 004, India

Received 18 January 1989; revised 25 October 1989

Data collected on board *ORV Sagar Kanya* during August 1985 along the west of 60°E meridian between 4°N and 6°S latitude indicate considerable difference in nutrient and dissolved oxygen (DO) content in the upper 200 m layer. Warm and nutrient rich water with low oxyty has been observed along 60°E meridian in contrast to the cold and relatively nutrient deficient water with high oxygen to the west of it. In addition, the existence of warm waters with high nutrients and low DO in the north and relatively cold water with low nutrients and high DO in the south is observed. The relationship of DO with nutrients shows a significant negative correlation. The inter-relationship of nutrients, PO₄-P and NO₃-N gives atomic ratios of 12.3:1 and 9.7:1 along section I and II respectively, while SiO₄-Si-σt relationship used for characterizing the watermasses indicates the presence of Arabian Sea surface water, the Pacific water and the Red Sea water along these 2 sections.

Western Indian Ocean is one of the important regions due to the presence of Somali current and the occurrence of upwelling in the far west. These features are more pronounced during the SW monsoon¹⁻³.

Most of the studies conducted in the equatorial western Indian Ocean pertain to the physical oceanographic parameters⁴⁻⁷ and information on chemical aspects⁸⁻¹¹ is lacking. In view of this, study on chemical aspect has been undertaken in the equatorial region of the western Indian Ocean during August 1985 to understand the distribution and chemistry of nutrients and the watermass structure.

Materials and Methods

Following the conventional procedures, water samples were collected at standard depths within the upper 1000 m. These collections were made at 21 stations along two sections, (I) parallel to the Somali coast and runs across the equator between 48°E and 53°E and (II) along 60°E meridian (Fig. 1). Nutrients were analysed on board with the help of Skalar 6-channel auto-analyser (5100/1) and dissolved oxygen (DO) was estimated by the modified Winkler's method¹².

Results and Discussion

Temperature—Along section I, the surface temperature varies from 25.08° to 26°C with mixed layer depth fluctuating from 30 m at 3°S (st 75) to

100 m near the equator (st 69); it shows a shallowing tendency on either side of the equator. At st 75, the spreading of isotherms is observed in the upper 200 m (Fig. 2a).

Along section II, the surface temperature varies from 26.61° (st 114) to 29.02°C (st 98). The mixed layer (approx. 75 m thick) is well developed on the southern half of the section. However, at st 108 the isotherms present a V-shape in contrast to an inverted V-shape at st 96 in the north (Fig. 2b). Below 200 m the temperature distribution in both the sections is nearly uniform.

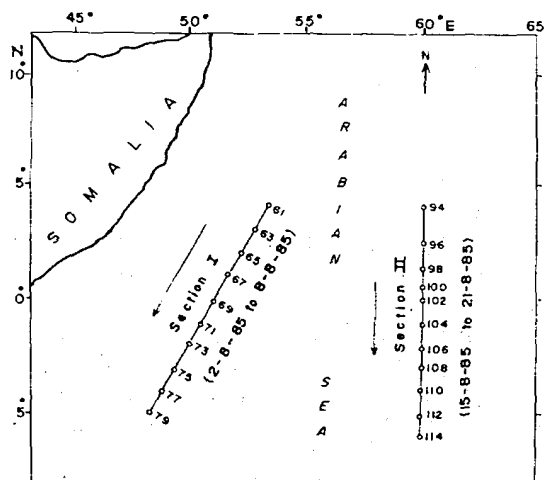


Fig. 1—Location of stations

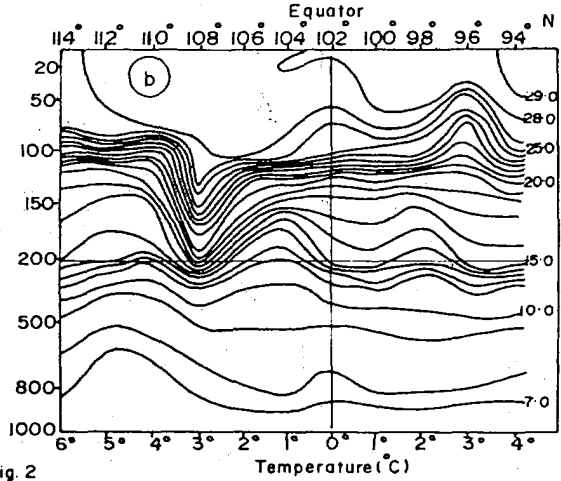
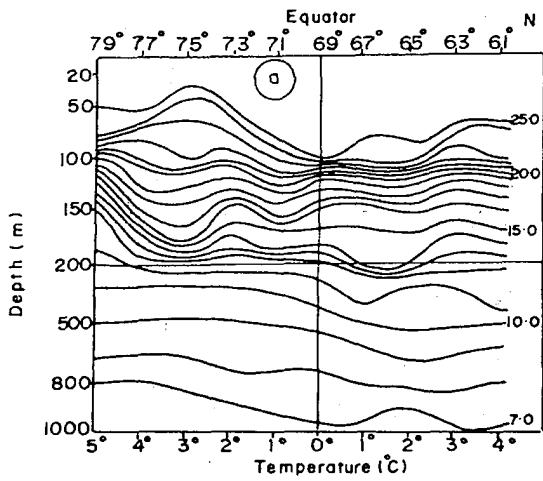


Fig. 2

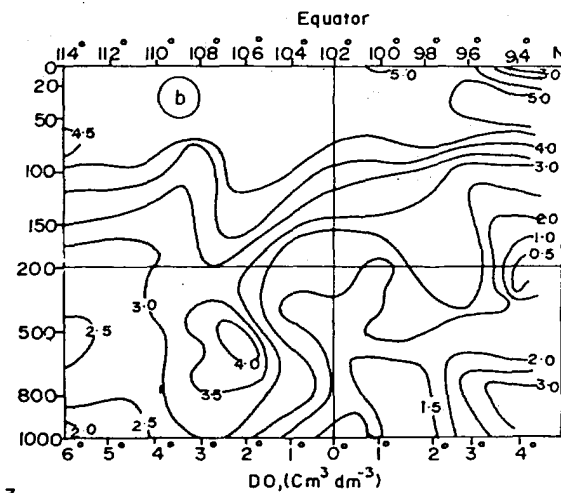
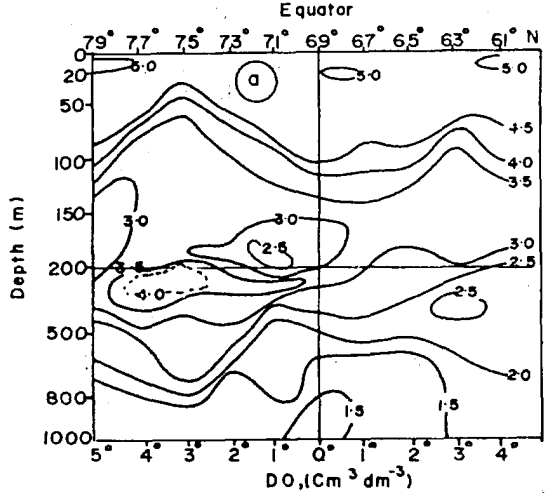


Fig. 3

Fig. 2—Vertical profiles of temperature along sections I(a) and II(b)

Fig. 3—Vertical profiles of DO along sections I(a) and II(b)

The observed spatial variation in temperature is due to the variable intensities of prevailing currents and the consequent mixing of water which is a result of circulation in the monsoon gyre, in which case the surface currents along the equator are predominantly eastward with convergence in the surface layer^{13,14}. The spreading of isotherms can be mainly due to the current-shear that exists between two opposing currents¹⁵.

Dissolved oxygen—DO content (Fig. 3a,b) does not exhibit appreciable variations within the top 50 m though changes do occur from west to east below the depth of 100 m in addition to meridional variations at all depths.

In section I, DO varies from 4.55 to 4.80 $\text{cm}^3 \text{dm}^{-3}$ in the upper 50 m and the isopleths indicate

step gradients in the depth layer 75-125 m below which the distribution becomes more irregular (Fig. 3a). Along st 63 and st 75, dome shaped structures are seen in the upper 75 m. Around st 75 fairly thick column of water with oxygen values from 3-4 $\text{cm}^3 \text{dm}^{-3}$ extends up to 500 m depth. However, the same water column has low DO around st 63. A layer of low oxygen (2.5 $\text{cm}^3 \text{dm}^{-3}$) is observed around st 71 in 180-200 m depth range and high DO (4.0 $\text{cm}^3 \text{dm}^{-3}$) is observed between st 73 and st 77 within 200-350 m depth.

In section II, the top 30 m water column with low DO (3-4 $\text{cm}^3 \text{dm}^{-3}$) is observed at st 94 (Fig. 3b). The surface of high concentrations of DO slopes down to 1000 m depth between st 106 and-st 108 while maximum DO is present at 500-700 m. At st

94 around 200 m, the minimum oxygen content, $0.5 \text{ cm}^3 \text{ dm}^{-3}$, is noticed. The isopleths of higher concentrations of DO present in the upper 200 m water column in the north deepen in the south of the equator.

The observed high oxygen ($4 \text{ cm}^3 \text{ dm}^{-3}$) around st 75 and st 77 along section I within 200-300 m depth may be due to the strong easterly current. The alternate bands of easterly and westerly flows on either side of the equator were observed by Suryanarayanan *et al.*¹⁶ throughout the 500 m water column.

Due to the spreading and deepening of isotherms along st 75 and st 108 in section I and II respectively, the isolines of oxygen also tend to spread and deepen within the 500 m water column in that region.

Phosphate-phosphorous ($\text{PO}_4\text{-P}$)—The concentrations of $\text{PO}_4\text{-P}$ are higher in section II as compared to section I and below 100 m, $\text{PO}_4\text{-P}$ shows almost two fold increase in section II.

In section I, the surface layer shows low $\text{PO}_4\text{-P}$ concentration ($0.02 \mu \text{ mol dm}^{-3}$) which gradually increases to $0.5 \mu \text{ mol dm}^{-3}$ at 100 m (Fig. 4a). Around 200-300 m depth $\text{PO}_4\text{-P}$ increases to $1 \mu \text{ mol dm}^{-3}$ while at 1000 m the highest concentration of $2.5 \mu \text{ mol dm}^{-3}$ is observed. In section II, the surface layer shows $\text{PO}_4\text{-P}$ varying from 0.1-0.5 $\mu \text{ mol dm}^{-3}$. At st 98 around 2°N , high $\text{PO}_4\text{-P}$ concentration ($2 \mu \text{ mol dm}^{-3}$) is seen within the top 50 m layer while between st 104 and st 106 low values of $\text{PO}_4\text{-P}$ extend down to 800 m.

Nitrate-nitrogen ($\text{NO}_3\text{-N}$)—Along section I, very low concentrations of $\text{NO}_3\text{-N}$ ranging from 0.0-0.8 $\mu \text{ mol dm}^{-3}$ are noticed in the upper 50 m layer

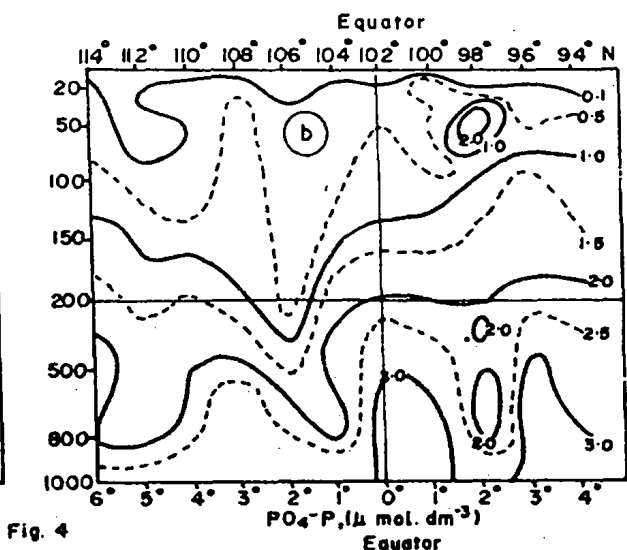
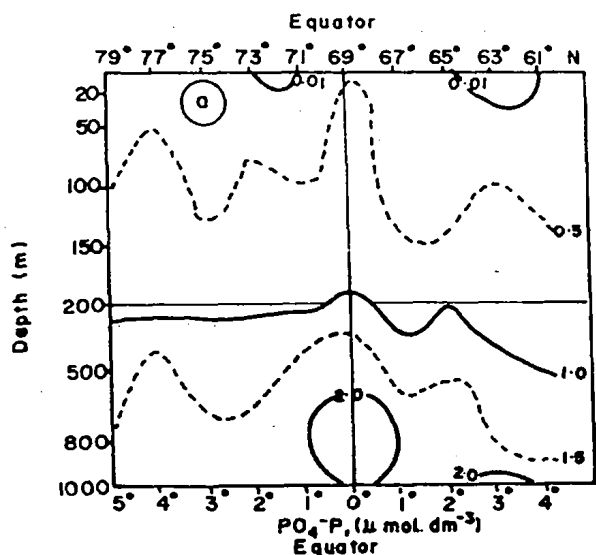


Fig. 4

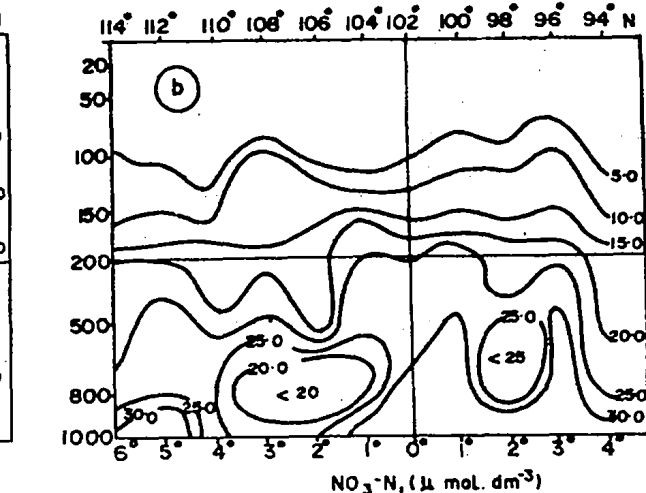
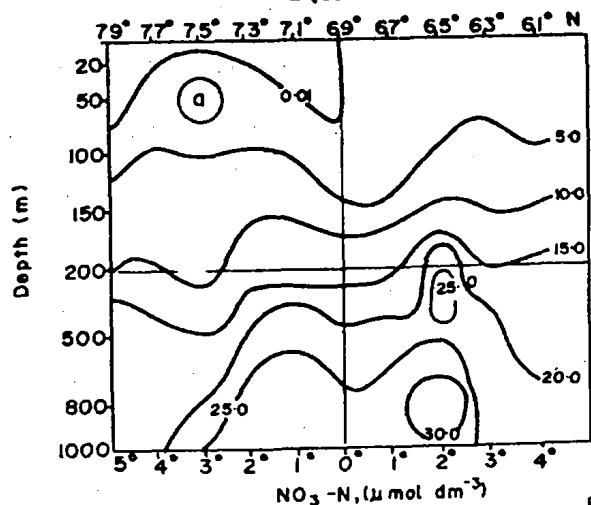


Fig. 5

Fig. 4—Vertical profiles of phosphate along sections I(a) and II(b)

Fig. 5—Vertical profiles of nitrate along sections I(a) and II(b)

(Fig. 5a), below which it gradually increases downward and shows the highest concentration $30 \mu \text{mol dm}^{-3}$ in the depth range 400-1000 m along st 65. Along section II (Fig. 5b) nitrate of very low concentration ($0.2 \mu \text{mol dm}^{-3}$) is observed while in the upper 75 m. The concentrations thereby increase downwards up to 1000 m as in section I. Around st 104-st 110 and st 98 between 700 and 800 m depth layer low values of nitrate are noticed, while highest ($33.9 \mu \text{mol dm}^{-3}$) values are observed at 1000 m around st 112-st 114.

Silicate—Section I (Fig. 6a) shows significantly low concentrations in the top 30 m with gradually increasing concentrations at depth. At 125 m, values as high as $10 \mu \text{mol dm}^{-3}$ are observed while at 200 m, the concentrations become double ($20\text{--}25 \mu \text{mol dm}^{-3}$). At 1000 m, silicate shows higher values of $75 \mu \text{mol dm}^{-3}$.

In section II (Fig. 6b), in the upper 75 m silicate shows uniformly low and negligible concentrations which increase gradually from very low value at 75 m to about $5 \mu \text{mol dm}^{-3}$ at 100 m near the equator. At st 110 isolines of high concentrations of silicate shoal upward to 100 m from 150 m depth. Around st 96 the highest concentration of about $100 \mu \text{mol dm}^{-3}$ are observed at 1000 m.

Pooled values of temperature, DO and nutrients (Table 1) show an increase in nutrients and a decrease in DO towards north relative to south across the equator. Moreover in section I, the surface water is relatively cold (25°C) with high DO, low nutrients and low silicates while in section II, the surface water is warmer (27.5°C) with low DO, high nutrients and high silicates.

The north-south difference could be due to the variation in water mass composition while the low surface temperature observed at section I is due to the proximity of section I to the source region of the cold upwelled water¹⁷.

DO shows a negative correlation with nutrients ($r = -0.85$ and -0.86 for $\text{PO}_4\text{-P}$ and $\text{NO}_3\text{-N}$ respectively along section I and $r = -0.8$ each for $\text{PO}_4\text{-P}$ and $\text{NO}_3\text{-N}$ along section II). Moreover, along section II the maximum oxygen content is marked by minimum content of $\text{PO}_4\text{-P}$ and $\text{NO}_3\text{-N}$ and vice-versa. This indicates that mostly the dissolved oxygen at these depths is utilized to breakdown organic matter and release nutrients.

Relationship between nitrate and phosphate is deduced by plotting the values of $\text{NO}_3\text{-N}$ against those of $\text{PO}_4\text{-P}$ in the depth range 75-1000 m separately for each section. The plots gave 2 different slopes of regression lines. For section I, the slope is 12.3 while for section II it is 9.7 with correlation coefficients $r = 0.88$ and 0.87 respectively. The ob-

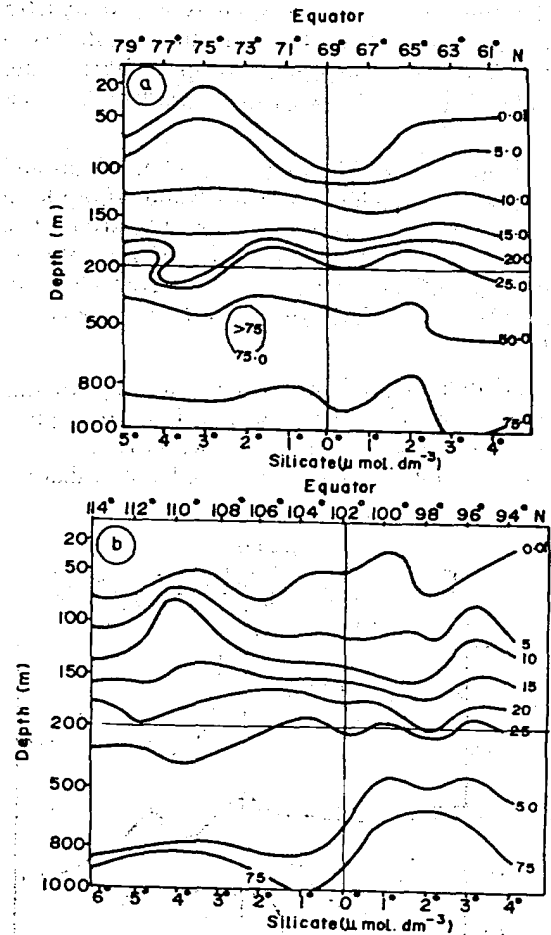


Fig. 6—Vertical profiles of silicate along sections I(a) and II(b)

served ratios of 12.3:1 and 9.7:1 along section I and II respectively are significantly lower than the theoretical one ($\text{N:P} = 16:1$)¹⁸. This alteration in ratio appears to be partly due to an increase of $\text{PO}_4\text{-P}$ in this region.

The classification of water mass from 0-1000 m is made on the basis of silicate-density ($\text{SiO}_4\text{-Si-}\sigma_t$) relationship as suggested by Steffansson and Atkinson¹⁹ and by Wooster *et al.*²⁰.

The water along sections I and II from 0-100 m shows σ_t between 22 and 26 with silicate concentrations varying from 0-10 $\mu \text{mol dm}^{-3}$. The salinity of this water as reported earlier¹⁶ is high ($35.1\text{--}35.9 \times 10^{-3}$). This water also has a higher temperature. This layer of water therefore largely includes the Arabian Sea surface water.

Below 200 m, silicate increases linearly from 20-60 $\mu \text{mol dm}^{-3}$ with depth up to 500 m with σ_t varying from 26-26.9. The salinity of this water¹⁶ to the south of the equator is $< 35 \times 10^{-3}$ varying from 34.8 to 35.0×10^{-3} while it is $> 35 \times 10^{-3}$ to the

Table 1—Pooled values of temperature, DO and nutrients along sections I and II

Depth (m)	Temperature °C			Dissolved Oxygen (cm ³ .dm ⁻³)			PO ₄ - P (μ mol dm ⁻³)			NO ₃ - N (μ mol dm ⁻³)			Silicate (μ mol dm ⁻³)			
	North	South	Av	North	South	Av	North	South	Av	North	South	Av	North	South	Av	
0	I	25.53	25.47	25.55	4.75	4.84	4.75	0.053	0.14	0.03	0.625	0.032	0.25	0.02	0.025	0.023
	II	28.19	27.43	27.76	4.21	4.49	4.58	0.000	0.00	0.00	0.000	0.000	0.00	0.006	0.002	0.003
10	I	25.55	25.37	25.49	4.86	4.81	4.82	0.250	0.158	0.189	0.625	0.037	0.25	0.02	0.026	0.023
	II	28.19	27.35	27.79	4.72	4.79	4.70	0.250	0.070	0.150	0.000	0.000	0.000	0.026	0.00	0.013
20	I	25.54	25.44	25.52	4.83	4.86	4.86	0.15	0.198	0.200	0.625	0.117	0.290	0.019	0.026	0.023
	II	28.19	27.47	27.72	4.79	4.85	4.81	0.233	0.220	0.230	0.000	0.000	0.000	0.00	0.00	0.00
30	I	25.51	25.39	25.47	4.72	4.68	4.69	0.123	0.258	0.211	0.625	0.310	0.390	0.00	0.227	0.113
	II	28.20	27.47	27.77	4.60	4.83	4.75	0.680	0.220	0.000	0.000	0.000	0.000	0.02	0.227	0.124
50	I	25.48	24.87	25.21	4.72	4.61	4.64	0.133	0.320	0.280	1.050	1.150	0.980	0.00	1.041	0.53
	II	27.67	27.35	27.51	4.99	4.79	4.86	1.120	0.190	0.490	0.050	0.090	0.050	0.75	0.00	0.38
75	I	25.04	23.75	24.46	4.39	3.98	4.21	0.233	0.34	0.320	2.780	2.370	2.280	2.01	4.01	3.01
	II	25.44	27.13	26.50	3.99	4.61	4.34	0.75	0.30	0.510	1.930	0.310	1.100	1.25	2.75	2.00
100	I	23.95	21.54	22.86	3.97	3.62	3.85	0.267	0.522	0.380	5.350	4.880	4.600	4.34	7.00	5.67
	II	23.23	24.23	24.39	3.41	4.38	4.01	1.050	0.450	0.700	7.500	3.610	5.120	4.75	3.75	4.25
200	I	14.00	12.96	13.40	2.75	2.64	2.71	0.833	0.834	0.840	16.900	10.800	13.310	28.00	22.80	25.40
	II	14.73	14.24	14.19	1.98	2.70	2.38	2.130	1.240	1.690	21.68	15.75	18.830	24.75	22.25	23.50
300	I	11.75	11.01	11.31	2.64	3.51	3.14	1.000	0.982	1.020	19.730	12.000	15.210	35.33	27.80	31.47
	II	12.31	11.65	12.00	1.86	2.68	2.30	2.380	1.480	1.900	23.880	19.900	21.860	29.75	23.50	26.82
400	I	11.00	9.93	10.37	2.42	3.71	3.10	1.10	1.12	1.15	22.300	13.910	17.730	47.33	40.00	43.86
	II	10.79	10.13	10.43	1.98	2.59	2.24	2.48	1.95	2.27	24.830	23.450	24.380	35.00	30.50	32.75
500	I	10.41	9.32	9.70	2.25	2.94	2.61	1.23	1.34	1.33	21.630	17.360	19.280	54.87	64.80	59.73
	II	10.16	9.18	9.65	2.07	3.00	2.54	2.70	1.98	2.330	26.600	24.400	25.570	43.00	36.00	35.50
800	I	8.57	7.95	8.32	1.97	2.07	1.76	1.57	1.60	1.650	25.400	21.480	23.520	61.87	55.75	80.71
	II	8.38	7.32	7.89	1.80	2.89	2.29	2.73	2.03	2.470	26.850	21.180	24.840	58.25	24.67	41.46
1000	I	7.00	—	7.00	1.75	1.97	1.64	1.93	1.73	1.810	25.550	22.530	24.160	74.00	82.33	78.16
	II	6.80	6.34	6.63	2.13	2.31	2.12	3.13	2.48	2.870	30.600	27.200	29.370	87.00	86.34	86.66

north of the equator, varying from $35-35.25 \times 10^{-3}$. This layer of water in general has a low temperature and shows a considerable decrease towards south of the equator as compared to the north. At intermediate depths in the Somali basin the water mass structure is very disorderly due to intermixing of water masses at various levels¹⁷. Tchernia *et al.*²¹ have indicated the horizontal distribution of salinity in the Somali basin to show a relatively fresh core within the south equatorial current emanating from the eastern archipelago with a 400 m salinity that still remains as low as 34.6×10^{-3} . This water comes southward from the Pacific equatorial currents by way of Banda Sea and penetrates the more saline Indian water as far as 60°E where its salinity still remains as low as 34.9×10^{-3} . Sharma *et al.*²² while working in the Western Indian Ocean have shown the incursion of low salinity water in this region in the south. All these features show that the southern region represents a different water mass or rather an intrusion of water of low salinity. This water therefore can probably be the Pacific water.

Lastly, the water between 500-1000 m shows high σ_t ranging from 27-27.5 with silicate varying

from 60-100 μ mol dm⁻³. The salinity of this layer of water¹⁶ is also found to be $> 35 \times 10^{-3}$. This water has low temperature and can be said to be the Red Sea water.

Acknowledgement

The authors are grateful to Dr B N Desai, Director and to Dr R Sen Gupta, Head, Chemical Oceanography Division for encouragement.

References

- 1 Szekiela K H, *The development of upwelling along the Somali coast as detected with the Nimbus 2 and Nimbus 3 satellites*, Tech Publ X-651-70-419 (Goddard Flight Centre, Greenbelt) 1970, 52.
- 2 Fieux M & Levy C, in *Hydrodynamics of the equatorial ocean*, edited by J C Nihoul (Elsevier, New York) 1983, 17.
- 3 Wyrki K, in *The biology of the Indian Ocean*, edited by B Zeitzschel (Springer-Verlag, Berlin) 1973, 18.
- 4 Swallow J C, *Deep-Sea Res*, 31 (1984) 639.
- 5 Reverdin G & Fieux M, *Deep-Sea Res*, 34 (1987) 601.
- 6 Luyter J R, Fieux M & Gonella J, *Science Wash.* 209 (1980) 600.
- 7 Sastry J S, Premchand K & Murty C S, *Mausam*, 37 (1986) 107.
- 8 Ryther J H, Hall J R, Pease A K, Bakun A & Jones M M, *Limnol Oceanogr.* 11 (1966) 371.

- 9 Fraga F, *Deep-Sea Res*, 13 (1966) 413.
- 10 Mc Gill D A, in *The biology of the Indian Ocean*, edited by B Zeitzschel (Springer-Verlag, Berlin) 1973, 53.
- 11 Sen Gupta R, George M D & Qasim S Z, *Indian J Mar Sci*, 5 (1976) 201.
- 12 Carritt D E & Carpenter J H, *J Mar Res*, 24 (1966) 286.
- 13 Swallow J C & Bruce J G, *Deep-Sea Res*, 13 (1966) 861.
- 14 Bruce J G, *J Geophys Res*, 78 (1973) 6386.
- 15 Pickard G L & Emery W J, in *Descriptive physical oceanography* (Pergamon Press, Oxford) 1968, 193.
- 16 Suryanarayanan A, Reddy G V & Pankajakshan T, *Di Hydrogr Z*, 40 (1987) 181.
- 17 Warren B, Stommel H & Swallow J C, *Deep-Sea Res*, 13 (1966) 825.
- 18 Takahashi T, Broecker W S & Langer S, *J Geophys Res*, 90 (1985) 6907.
- 19 Steffansson U & Atkinson L P, *Limnol Oceanogr*, 16 (1971) 51.
- 20 Wooster W S, Schaefer M B & Robinson M K, Institute of Marine Resources, San Diego, California, 1967, 67 (mimeo).
- 21 Tchernia P, Lacombe H & Guibout P, *Bull Inf Com Cent Oceanogr Etude Cotes*, 10 (1958) 115.
- 22 Sharma G S, Gouveia A D & Satyendranath S, *Proc Indian Acad Sci (E & P Sciences)*, 87 (1978) 29.